Semiconductor Physics, Quantum Electronics & Optoelectronics, 2023. V. 26, No 2. P. 159-164.

Semiconductor physics

Kinetics of charge carriers in bilateral macroporous silicon

V.F. Onyshchenko, L.A. Karachevtseva, K.V. Andrieieva, N.V. Dmytruk, A.Z. Evmenova

V. Lashkaryov Institute of Semiconductor Physics, National Academy of Sciences of Ukraine
41, prosp. Nauky, 03680 Kyiv, Ukraine
**Corresponding author e-mail: onyshchenkovf@isp.kiev.ua*

Abstract. The kinetics of charge carriers in bilateral macroporous silicon with macroporous layers of equal thicknesses is calculated by the finite difference method. A diffusion equation for a monocrystalline substrate and macroporous layers is solved. The boundary conditions are defined at the boundaries between the monocrystalline substrate and the macroporous silicon layers on both sides. Stationary distribution of excess charge carriers in the bilateral macroporous silicon with the macroporous layers of equal thicknesses calculated by the finite difference method is set as the initial condition. Under stationary conditions, excess charge carriers are generated by light with the wavelengths of 0.95 μm and 1.05 μm. It is shown that at the counting times much longer than the relaxation time, all the distributions of the concentration of excess minority carriers generated by light with any wavelength approach the same distribution with exponentially decreasing value.

Keywords: kinetics, relaxation, distribution of excess charge carriers, bilateral macroporous silicon.

https://doi.org/10.15407/spqeo26.02.159
PACS 85.30.De, 85.60.Jb

Manuscript received 12.12.22; revised version received 29.04.23; accepted for publication 07.06.23; published online 26.06.23.

1. Introduction

Macroporous silicon finds application as photonic crystals, for chemical sensors, photodetectors, solar cells and a number of other types of detectors and sensors. Photonic crystals have band gaps enabling light transmission. They are characterized by a periodic change of the dielectric constant with the period comparable to the light wavelength. The periodicity of the permittivity of such crystals is created by periodically located macropores. Three-dimensional macroporous silicon photonic crystals with large areas were fabricated and studied [1, 2]. Macroporous silicon is also applied for gas sensing. A miniature gas sensor for detecting carbon dioxide was created based on macroporous silicon [3, 4]. A sensor for measuring refractive index was made based on arrays of microsensors placed on a macroporous silicon membrane filled with a liquid [5]. Macroporous silicon with an adjustable array of macropores was coated with a multilayered antireflection coating, which turned it into black silicon having high light absorption [6]. Photoluminescence of macroporous silicon structures with SiO_2 layers was measured. The maximum photo-luminescence was observed in the samples with high electric field strength at the interface between the macroporous silicon and SiO_2 [7].

Further applications of macroporous silicon include textured crystalline silicon solar cells. The efficiency of using the energy produced by such cells and their power was optimized with a monitoring and control system, which made it possible to optimize the solar cell area and a number of other key parameters [8]. Energy savings were achieved by using LED lighting in combination with solar panels [9]. The photoconversion efficiency and short circuit current of crystalline textured silicon solar cells were calculated using a theoretical model enabling optimization of these characteristics. The theoretical model takes into account the recombination mechanisms in the space charge region and in the solar cell bulk [10, 11]. The change of the concentration of excess charge carriers in bilateral macroporous silicon in the direction parallel to the pores was calculated. The calculations were made for different pore depths in each macroporous layer. The distribution of the concentration of excess charge carriers in bilateral macroporous silicon depended on the bulk lifetime of minority carriers, sample thickness and pore diameter and depth. The dependence of the excess carrier concentration in bilateral macroporous silicon with different thicknesses of the macroporous layers had one or two maxima. Two maxima were observed illuminating the sample with light

with the wavelength of 0.95 μm close to the illuminated sample surface and the single crystal substrate. One maximum was observed in the middle of the substrate when the sample was illuminated with light with the wavelength of 1.05 μm [12]. The effective lifetime of minority charge carriers was calculated for macroporous silicon on a monocrystalline substrate and macroporous silicon with through pores. The surface recombination velocity on the macroporous silicon surface was calculated from the pore morphology data [13]. The effective lifetime of charge carriers in the bilateral macroporous silicon was found from two equations obtained by solving the diffusion equation for minority carriers in the macroporous layers and monocrystalline substrate. The boundary conditions for the diffusion equation were defined at the boundaries between the macroporous silicon layers and the monocrystalline substrate. Each equation describes the processes in the macroporous layer and at the boundary between the macroporous layer and the monocrystalline substrate. The effective lifetime of minority charge carriers in the bilateral macroporous silicon was calculated as a function of macropore depth [14]. The photoconductivity in the porous and macroporous silicon was calculated numerically and analyzed analytically [15]. The kinetics of photoconductivity in the bilateral macroporous silicon was calculated as a function of macropore depth in the front or back macroporous layer. Calculations show that the period of the initial photoconductivity decay increases with the increase of the front or back macroporous silicon layer thickness. The photoconductivity kinetics in macroporous silicon with through pores follows an exponential law [16].

The purpose of this work is to calculate and analyze the charge carrier kinetics in bilateral macroporous silicon with equal thicknesses of the macroporous layers. We calculate the dependence of the concentration of excess minority carriers on the coordinate and time by the finite difference method. The results of this work will be useful for researchers of bilateral macroporous silicon developing photodetectors, solar cells and sensors on its base.

2. Charge carrier kinetics in bilateral macroporous silicon

The diffusion equation for minority charge carriers under stationary conditions in the front macroporous layer (i = 1), monocrystalline substrate (i = 2) and back macroporous layer (i = 3) is written as follows:

$$D_p \frac{d^2\delta p_i(x)}{\mathrm{d}x^2} - \frac{\delta p_i(x)}{\tau_i} + g_{0p}(\alpha)\exp(-\alpha x)k_i = 0, \qquad (1)$$

where D_p is the diffusion coefficient of minority charge carriers, $\delta p_i(x)$ is the excess minority carrier concentration in the front macroporous layer (i = 1), monocrystalline substrate (i = 2) and back macroporous layer (i = 3), $\tau_2 = \tau_b$ is the bulk lifetime of minority carriers in the monocrystalline substrate (silicon single crystal), $\tau_i = 1\Big/\left(\frac{1}{\tau_b} + \frac{\pi D_{pori} s_{pori}}{a_i^2 - \pi D_{pori}^2/4}\right)$ (i = 1, 3), $g_{0p}(\alpha)$ is the surface generation rate of excess minority charge carriers, α is the absorption coefficient of silicon, $k_1 = 1$, $k_2 = k_3 = 1 + P_1(\exp(\alpha h_1) - 1)$, $P_1 = \pi(D_{por1}/(2a_1))^2$ is the volume fraction of pores, and h_1, D_{por1} and a_1 are the pore depth (thickness), pore diameter and the distance between the pore centers in the front macroporous layer, respectively.

The diffusion equation for minority charge carriers in the front macroporous layer (i = 1), monocrystalline substrate (i = 2) and back macroporous layer (i = 3) is written as follows:

$$\frac{\partial\delta p_i(x,t)}{\partial t} = D_p \frac{d^2\delta p_i(x,t)}{\mathrm{d}x^2} - \frac{\delta p_i(x,t)}{\tau_i}. \qquad (2)$$

The initial condition is defined as $\delta p_i(x, 0) = \delta p_i(x)$. The boundary conditions at the sample boundaries are set as follows:

$$D_p \frac{dp_1(0,t)}{\mathrm{d}x} = s_1 p_1(0,t), \qquad (3)$$

$$D_p \frac{dp_3(h,t)}{\mathrm{d}x} = s_2 p_3(h,t), \qquad (4)$$

where s_1 and s_2 are the surface recombination velocities on the front and back surfaces of the sample, respectively. The boundary conditions at the monocrystalline substrate boundaries look as follows:

$$(1-P_1)D_p \frac{dp_1}{\mathrm{d}x}(h_1,t) = D_p \frac{dp_2}{\mathrm{d}x}(h_1,t) - P_1 s_{por1} p_2(h_1,t), \qquad (5)$$

$$(1-P_2)D_p \frac{dp_3}{\mathrm{d}x}(h-h_2,t) = D_p \frac{dp_2}{\mathrm{d}x}(h-h_2,t) - P_2 s_{por2} p_2(h-h_1,t), \qquad (6)$$

where $P_2 = \pi(D_{por2}/(2a_2))^2$ is the volume fraction of pores, h_2, D_{por2} and a_2 are the pore depth (thickness), pore diameter and the distance between the pore centers in the back macroporous layer, respectively, and s_{por1} and s_{por2} are the surface recombination velocities on the surface of the pores in the front and back macroporous layer, respectively. The concentration of excess minority carriers should be continuous at the boundaries of the monocrystalline substrate:

$$p_1(h_1,t) = p_2(h_1,t), \qquad (7)$$

$$p_2(h-h_2,t) = p_3(h-h_2,t). \qquad (8)$$

Eqs (1) and (2) with the boundary conditions (3)–(8) are solved numerically using, *e.g.*, the finite difference method.

3. Results and discussion

We calculated the stationary distribution of the concentration of excess minority carriers in bilateral macroporous silicon when the excess charge carriers are generated by light illumination. The finite difference method was used to solve Eq. (1) with the boundary conditions (3)–(8) and the initial condition $\delta p_i(x) = \delta p_i(x, 0)$. The distribution of the concentration of excess minority carriers began to change with time after termination of generation of excess charge carriers. We calculated the kinetics of the distribution of the concentration of excess minority carriers in bilateral macroporous silicon by solving Eq. (2) with the boundary conditions (3)–(8) by the finite difference method. The initial distribution corresponded to the stationary conditions. The distribution was calculated for 500 μm thick bilateral macroporous silicon. The macropore depth in each macroporous layer was 100 or 200 μm, the average macropore diameter was 1 μm, and the average distance between the pore centers was 2 μm. The bulk lifetime of minority carriers in the monocrystalline substrate was 10 μs, which is a typical value for silicon wafers. The value of the bulk lifetime in single-crystalline silicon used for solar cell fabrication can vary from 1 μs to 5 ms [17] at a concentration of majority charge carriers of 10^{15} cm^{-3}. The effective bulk lifetime of excess charge carriers in each macroporous layer was calculated using the bulk lifetime and surface recombination velocity [14] and amounted to 1 μs. The surface recombination velocity on the pore surface in each macroporous layer and the surface of the macroporous silicon sample was 1 m/s. This value is typical for a well passivated surface of silicon macropores [13], although lower surface recombination velocities were also reported [18].

Fig. 1 shows the change of the concentration of excess minority carriers along the thickness of the bilateral macroporous silicon sample with the pore depth of 100 μm at certain times after termination of generation by light with the wavelength of 0.95 μm.

Two maxima on the concentration distribution of excess minority charge carriers in the bilateral macroporous silicon with the pore depth of 100 μm under stationary conditions, when the excess charge carriers are generated by light with the wavelength of 0.95 μm are observed (see Fig. 1, curve *1*). The stationary distribution is the initial one ($t = 0$). The maxima are observed at the surfaces hit by light, namely the sample surface and the surface of the monocrystalline substrate (pore bottom surface). Light enters the monocrystalline substrate through the front macroporous layer illuminating the bottom of the pores. This means that the value of the maximum located in the monocrystalline substrate depends on the pore depth in the front macroporous layer, the pore volume fraction and the recombination velocity on the sample and pore surfaces.

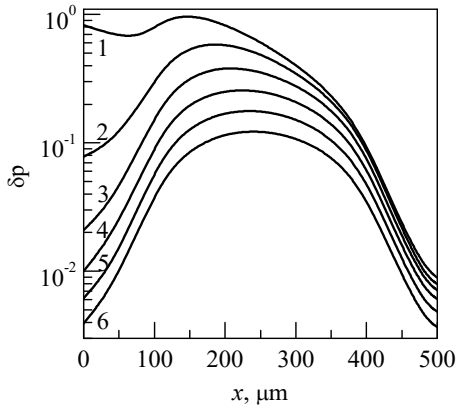

Fig. 1. Change of the concentration of excess minority carriers along the thickness of the sample with the pore depth of 100 μm after termination of generation (λ = 0.95 μm) at the times, μs: *1* – 0, *2* – 2, *3* – 4, *4* – 6, *5* – 8, *6* – 10.

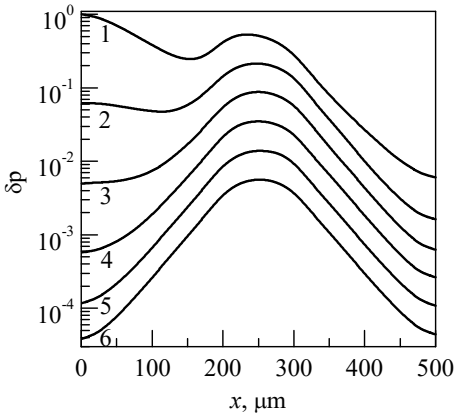

Fig. 2. Change of the concentration of excess minority carriers along the thickness of the sample with the pore depth of 200 μm after termination of generation (λ = 0.95 μm) at the times, μs: *1* – 0, *2* – 2, *3* – 4, *4* – 6, *5* – 8, *6* – 10.

Fig. 2 shows the change of the concentration of excess minority carriers along the thickness of the bilateral macroporous silicon sample with the pore depth of 200 μm at certain times after termination of generation by light with the wavelength of 0.95 μm.

In the initial distribution, the maximum located in the monocrystalline substrate is higher than the maximum located in the front macroporous layer when the pore depth in the latter is 100 μm (see Fig. 1) and lower when the pore depth is 200 μm (see Fig. 2). The concentration of excess minority carriers in the front macroporous layer rapidly decreases with time due to recombination at the pore surfaces. The concentration maximum rapidly decreases as well and disappears, so that only one maximum remains on the distribution of excess minority charge carriers in the bilateral macroporous silicon. The concentration of excess minority carriers in the monocrystalline substrate and its maximum decrease by the same amount in semi-logarithmic scale (exponential decrease). The concentration of excess

minority carriers decreases the faster, the closer it is to the front macroporous layer. Rapid decrease of this concentration in the front macroporous layer makes it ten (see Fig. 1) and one hundred (see Fig. 2) times smaller than the concentration in the monocrystalline substrate. At the beginning, the asymmetric concentration distribution transforms into a symmetric one (see Figs 1 and 2) defined by the symmetry of the macroporous silicon sample. All the asymmetric components of the concentration distribution rapidly decrease and become small, while the symmetric ones decrease slowly and exponentially.

Fig. 3 shows the change of the concentration of excess minority carriers along the thickness of the bilateral macroporous silicon sample with the pore depth of 100 μm at certain times after termination of generation by light with the wavelength of 1.05 μm.

The distribution of the concentration of excess minority carriers is almost symmetric about the middle of the sample having a maximum here. The symmetry of the distribution is due to the symmetry of the sample and uniformity of generation of excess charge carriers by light with the wavelength of 1.05 μm. Such light is weakly absorbed by silicon leading to homogeneous generation of excess charge carriers. Illumination of the monocrystalline substrate through the pores bottom does not affect the concentration distribution due to the weak absorption of light by silicon and small volume fraction of the pores. Although the distribution is symmetric, it changes over time.

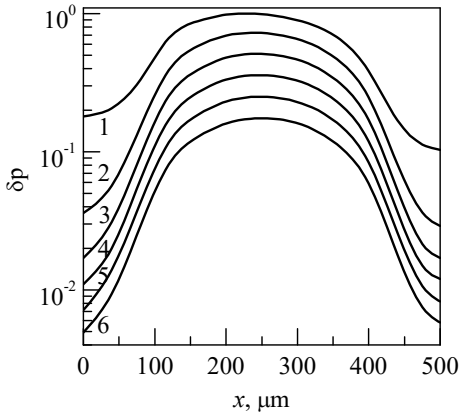

Fig. 3. Change of the concentration of excess minority carriers along the thickness of the sample with the pore depth of 100 μm after termination of generation (λ = 1.05 μm) at the times, μs: *1* – 0, *2* – 2, *3* – 4, *4* – 6, *5* – 8, *6* – 10.

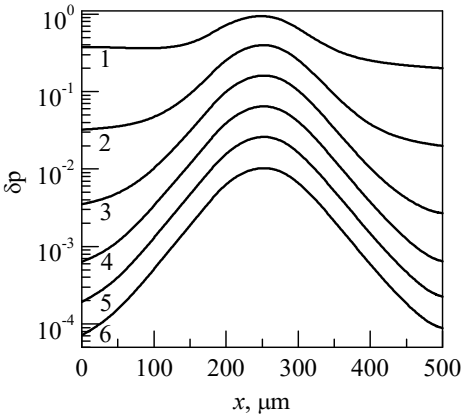

Fig. 4. Change of the concentration of excess minority carriers along the thickness of the sample with the pore depth of 200 μm after termination of generation (λ = 1.05 μm) at the times, μs: *1* – 0, *2* – 2, *3* – 4, *4* – 6, *5* – 8, *6* – 10.

Fig. 4 shows the change of the concentration of excess minority carriers along the thickness of the bilateral macroporous silicon sample with the pore depth of 200 μm at certain times after termination of generation by light with the wavelength of 1.05 μm.

As can be seen from Figs 3 and 4, the closer is the point to the front surface of the sample, the faster the concentration of excess minority carriers decreases with time becoming very small (faster than exponential decrease). In the back macroporous layer, the time dependence of the concentration of excess minority carriers is exponential. When the reference time is much longer than the relaxation time, all the distributions of the concentration of excess minority carriers (generated by light of any wavelength) approach the same distribution, the value of which decreases exponentially. This concentration distribution is determined by only the characteristics of the sample such as pore depth, surface recombination velocity, minority carrier bulk lifetime, pore diameter and distance between pores.

4. Conclusions

At the illuminated surface, the distribution of the concentration of excess minority carriers decreases faster than in the monocrystalline substrate. Due to this, this concentration at the surface quickly becomes very low as compared to the one in the monocrystalline substrate.

The concentrations of excess minority carriers in the monocrystalline substrate and in the front macroporous layer decrease exponentially almost from the very beginning. At this, the closer is the point to the front macroporous layer, the faster the concentration begins to decrease.

When the reference time is much longer than the relaxation time, all the distributions of the concentration of excess minority carriers generated by light with any wavelength approach the same distribution, the value of which decreases exponentially.

References

1. Matthias S., Hillebrand R., Müller F., Gösele U. Macroporous silicon: Homogeneity investigations and fabrication tolerances of a simple cubic three-dimensional photonic crystal. *J. Appl. Phys*. 2006. **99**, No 11. P. 113102. https://doi.org/10.1063/1.2200871.
2. Segura D., Vega D., Cardador D., Rodriguez A. Effect of fabrication tolerances in macroporous silicon photonic crystals. *Sens. Actuators A Phys.* 2017. **264**. P 172–179. https://doi.org/10.1016/j.sna.2017.07.011.

3. Pergand D., Geppert T.M., Rhein A. *et al*. Miniature infrared gas sensors using photonic crystals. *J. Appl. Phys*. 2011. **109**, No 8. P. 083117. https://doi.org/10.1063/1.3575176.
4. Maza D.C., Garcia D.S., Deriziotis I. *et al*. Empirical demonstration of CO_2 detection using macroporous silicon photonic crystals as selective thermal emitters. *Opt. Lett*. 2019. **44**, No 18. P. 4535–4538. https://doi.org/10.1364/OL.44.004535.
5. Seo S.-W., Azmand H.R., Enemuo A.N. Hollow core waveguide sensor array based on a macroporous silicon membrane structure. *J. Light. Technol*. 2019. **37**, No 9. P. 2036–2041. https://doi.org/10.1109/JLT.2019.2897427.
6. Ao X., Tong X., Kim D.S., *et al*. Black silicon with controllable macropore array for enhanced photoelectrochemical performance. *Appl. Phys. Lett*. 2012. **101**, No 11. P. 111901. https://doi.org/10.1063/1.4752231.
7. Karachevtseva L., Kuchmii S., Stroyuk A. *et al*. Light-emitting structures of CdS nanocrystals in oxidized macroporous silicon. *Appl. Surf. Sci*. 2016. **388**, Part A. P. 288–293. https://doi.org/10.1016/j.apsusc.2016.01.069.
8. Kornaga V.I., Pekur D.V., Kolomzarov Yu.V. *et al*. Intelligence system for monitoring and governing the energy efficiency of solar panels to power LED luminaires. *SPQEO*. 2021. **24**, No 2. P. 200–209. https://doi.org/10.15407/spqeo24.02.200.
9. Pekur D.V., Sorokin V.M., Nikolaenko Y.E. Features of wall-mounted luminaires with different types of light sources. *Electrica*. 2021. **21**, No 1. P. 32–40. https://doi.org/10.5152/electrica.2020.20017.
10. Sachenko A.V., Kostylyov V.P., Korkishko R.M. *et al*. Experimental investigation and theoretical modelling of textured silicon solar cells with rear metallization. *SPQEO*. 2022. **25**, No 3. P. 331–341. https://doi.org/10.15407/spqeo25.03.331.
11. Sachenko A.V., Kostylyov V.P., Korkishko R.M. *et al*. Simulation and characterization of planar high-efficiency back contact silicon solar cells. *SPQEO*. 2021. **24**, No 3. P. 319–327. https://doi.org/10.15407/spqeo24.03.319.
12. Onyshchenko V.F. Distribution of excess charge carriers in bilateral macroporous silicon with different thicknesses of porous layers. *J. Nano- Electron. Phys*. 2021. **13**, No 6. P. 06010. https://doi.org/10.21272/jnep.13(6).06010.
13. Ernst M., Brendel R. Modeling effective carrier lifetimes of passivated macroporous silicon layers. *Sol. Energy Mater. Sol. Cells*. 2011. **95**, No 4. P. 1197–1202. https://doi.org/10.1016/j.solmat.2011.01.017.
14. Onyshchenko V.F., Karachevtseva L.A. Effective minority carrier lifetime in double-side macroporous silicon. *SPQEO*. 2020. **23**, No 1. P. 29–36. https://doi.org/10.15407/spqeo23.01.29.
15. Monastyrskii L.S., Sokolovskii B.S., Pavlyk M.R. Analytical and numerical calculations of photoconductivity in porous silicon. *Ukr. J. Phys*. 2011. **56**, No 9. P. 902–906. https://doi.org/10.15407/ujpe56.9.902.
16. Onyshchenko V.F. Photoconductivity kinetics in bilateral macroporous silicon. *J. Nano- Electron. Phys*. 2022. **14**, No 5. P 05024. https://doi.org/10.21272/jnep.14(5).05024.
17. Measuring and interpreting the lifetime of silicon wafers. *Solar Energy*. 2004. **76**, No 1–3. P. 255–262. https://doi.org/10.1016/j.solener.2003.07.033.
18. Iandolo B., Sánchez Nery A.P., Davidsen R.S., & Hansen O. Black silicon with ultra-low surface recombination velocity fabricated by inductively coupled power plasma. *phys. status solidi – RRL*. 2019. **13**, No 2. P. 1800477. https://doi.org/10.1002/pssr.201800477.

Authors and CV

Volodymyr Onyshchenko, PhD in Physics and Mathematics, Senior Researcher at the V. Lashkaryov Institute of Semiconductor Physics, NAS of Ukraine. He is the author of more than 120 scientific publications. His main research interests include modelling photoconductivity kinetics in macroporous silicon.
https://orcid.org/0000-0002-4241-280X

Liudmyla Karachevtseva, Doctor of Technical Sciences, Professor, Leading Researcher at the V. Lashkaryov Institute of Semiconductor Physics, NAS of Ukraine. She is the author of more than 250 scientific publications. The area of her scientific interests includes photonic semiconductor structures, photoelectrochemistry, semiconductor physics, transport phenomena and recombination.
E-mail: larar@kartel.kiev.ua,
https://orcid.org/0000-0002-0709-325X

Kateryna Andrieieva, Researcher at the V. Lashkaryov Institute of Semiconductor Physics, NAS of Ukraine since 1999. The area of her scientific interests includes optoelectronic properties of narrow gap semiconductors, IR detectors, physics and technology of modern materials and devices.
E-mail: ev_andreeva322@ukr.net

Nadiia Dmytruk, Researcher at the V. Lashkaryov Institute of Semiconductor Physics, NAS of Ukraine. The area of her scientific interests includes physics and technology of modern materials.
E-mail: nvdmytruk@isp.kiev.ua

Anna Evmenova, Researcher at the V. Lashkaryov Institute of Semiconductor Physics, NAS Ukraine. She authored more than 40 publications and 4 patents. The area of her scientific interests includes physics and technology of semiconductor materials, heterostructures and devices (IR and THz detectors, nanomaterials *etc*.).
E-mail: evmenova_a@ukr.net,
http://orcid.org/0000-0001-8741-7498

Authors' contributions

Onyshchenko V.F.: methodology, writing – original draft, software, calculations.
Karachevtseva L.A.: conceptualization, supervision, project administration.
Andrieieva K.V.: formal analysis, writing – review & editing, software.
Dmytruk N.V.: writing – review & editing, visualization, data curation.
Evmenova A.V.: validation, visualization, formal analysis, calculations.

Кінетика носіїв заряду у двосторонньому макропористому кремнії

В.Ф. Онищенко, Л.А. Карачевцева, К.В. Андрєєва, Н.В. Дмитрук, А.З. Євменова

Анотація. Кінетика носіїв заряду у двосторонньому макропористому кремнії з однаковою товщиною макропористих шарів розраховується методом скінченних різниць. Ми використали рівняння дифузії, яке записали для монокристалічної підкладки та макропористих шарів. Граничні умови були записані на межах монокристалічної підкладки та зразка двостороннього макропористого кремнію. Як початкову умову ми використали розподіл надлишкових носіїв заряду у двосторонньому макропористому кремнії з однаковою товщиною макропористих шарів за стаціонарних умов, який розрахували методом скінченних різниць. За стаціонарних умов, світло з довжинами хвиль 0,95 мкм та 1,05 мкм генерувало надлишкові носії заряду. Показано, що коли час відліку буде набагато більшим за час релаксації, тоді всі розподіли концентрації надлишкових неосновних носіїв заряду, генерованих світлом з любою довжиною хвилі, перейдуть в один і той же розподіл, величина якого буде зменшуватись за експоненціальним законом.

Ключові слова: кінетика, релаксація, розподіл надлишкових носіїв заряду, макропористий кремній.